ELSEVIER

Journal of Nuclear Materials 266–269 (1999) 1023–1027

journal of nuclear materials

Thermal pattern measurements during disruptions on TEXTOR-94

M. Ciotti [a,*], T. Denner [b,1], G. Maruccia [c], K.H. Finken [b,1], J. Hobirk [b,1], A. Kremer-Flecken [b,1], G. Maddaluno [a], G. Mank [b,1], P. Pasqua [d], F.C. Schüller [e,1], R. Zanino [c]

[a] *Associazione EURATOM ENEA sulla fusione, C.E. Frascati, C.P. 65-00044 Frascati, Rome, Italy*
[b] *Institut fuer Plasmaphysik, Forschungszentrum Jülich, GMbH Association EURATOM-KFA, Jülich, Germany*
[c] *Dipartimento di Energetica, Politecnico, I-10129 Torino, Italy*
[d] *Dipartimento di Ingegneria Aerospaziale, Università di Roma 'La Sapienza', Roma, Italy*
[e] *FOM-Instituut voor plasmafysica 'Rijnhuizen', Ass EURATOM-FOM, Nieuwegein, The Netherlands*

Abstract

The thermal pattern onto the TEXTOR-94 toroidal limiter at the thermal quench for a set of four disruptions has been measured. A high temporal and spatial resolution camera, based on an infra-red 128 × 128 pixels focal plane array detector has been used to perform the measurements. Comparing the power profile for the same discharge as inferred from two images taken just before the disruption and at the thermal quench, it is possible to assess that: the radial exponential decay of the power flowing onto the limiter shows in both cases two different e-folding lengths; a short one (of the order of 2 mm or even less, in disruptive discharges) in the first few mm of the SOL depth and a larger one (1.5 cm) deeper in the SOL. An energy balance has been performed based on thermal images of both the limiter and the nearby wall during the thermal quench. The total energy lost is comparable to the plasma energy content.

Keywords: Disruption; e-folding length; Heat flux; Infra-red; Limiter; Power flux; Radiation loss; SOL power; TEXTOR; Thermal load; Thermal quench

1. Introduction

Disruptions are one of the main problems for existing and future tokamaks. During the thermal quench phase, usually lasting less than 1 ms, a huge power is released onto the first wall components [1]. In ITER, up to 100 GW/m^2 are expected, and whether the power spatial distribution changes with respect to the normal phase or not, is a crucial issue both in order to understand transport mechanisms and to plan first wall components and their lifetime. TEXTOR-94 is equipped with a toroidal belt pump-limiter (ALT-II) [2] positioned outboard at 45° below the mid plane; the major radius is 1.75 m and the minor is 0.46 m. The ALT-II limiter consists of eight blades covered with graphite tiles in two rows. Tiles have a thickness of up to 0.02 m; the last closed flux surface is intersected in the central line of the blades. Comparisons of the limiter thermal load and power decay length (λ_q) during the thermal quench phase of disruptions and the normal phase have been carried out. The aim of this contribution is to compare the spatial distribution of the power impinging onto the limiter during the thermal quench and the stationary phase, in order to show whether the magnetic configuration is preserved or not.

2. Experimental apparatus

A new infra-red (IR) system [3,4] has been installed on the TEXTOR-94 machine in the framework of a

* Corresponding author. E-mail: ciotti@frascati.enea.it.
[1] Partner in the Trilateral Euregio Cluster (TEC).

0022-3115/99/$ – see front matter
PII: S0022-3115(98)00559-5

collaboration between ENEA Frascati and KFA IPP Jülich. The system is based on a 2D Indium Antimonide (InSb) focal plane array with 128 × 128 pixels cooled at liquid nitrogen temperature that can be read up to 1100 frames/s. Up to 512 full frame images can be acquired as described in Refs. [3,4]. For the experiment performed the camera has been run at 1000 frames/s, in order to have at least half second of acquisition time to catch the disruption. The camera is equipped with a 4.74–4.95 μm filter instead of the standard 3.0–5.0 μm in order to increase the temperature range that can be measured without changing the electronic set up [5]. The field of view is of the order of 60 cm allowing to image one full limiter blade and a part of the wall, as shown in Fig. 1. This figure refers to an image taken at the thermal quench time.

To speed up the acquisition a four channels parallel reading is used, where two odd and two even pixels belonging to a couple of successive rows are read contemporaneously. The reading time of each couple of rows is negligible (12 μs) with respect to the thermal quench duration. Integration time can be set between 1% and 99% of the frame time depending on photon flux impinging on to the detector; this determines the number of pixels that are integrating at the same time as shown in Fig. 2; in our case, due to the high starting limiter temperature (over 300°C) the integration time is only 3% of the frame time and only two couples of rows are integrating at a time.

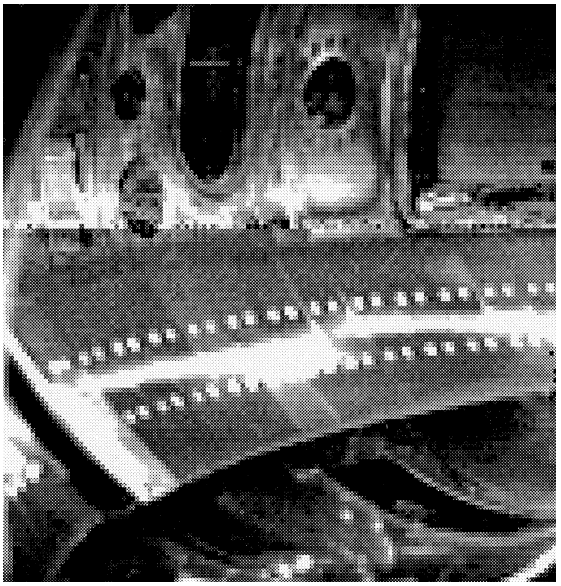

Fig. 1. The limiter blade imaged by the camera; it is possible to see a brighter zone just over the limiter corresponding to the thermal quench starting time.

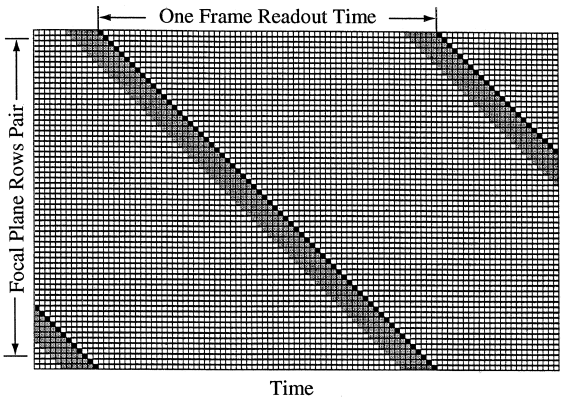

Fig. 2. The IR system row integration sequence. The frame readout time is divided into 64 parts. For each row pair, one part (black quad) is kept for readout. Dark grey quad shows that the row pair is integrating. The frame time fraction dedicated to integration is equal to ratio between the grey quad number and 64. In this example, the integration time is the 9.5% of frame time. For TEXTOR-94 measurements, we have used an integration time of 3% of frame time. White quad indicates that the row pair is idle.

3. Data elaboration

As can be seen in Fig. 1 a complicated heating pattern is observed on the limiter blade. This is mainly due to the composition of the toroidal field ripple and the limiter shape. Two misaligned tiles also cause local shadowing. The holes in the tiles where the tightening screws are located are also brighter due to their sharp edge. It is difficult to select several profiles where it is possible to calculate the λ_q, so that calculation has been done for several positions but skipping the anomalous pixels.

3.1. Stationary phase

The heat flux impinging onto the limiter in the stationary phase i.e., 1 ms before the thermal quench, has been obtained performing a complete 2D simulation by means of the finite elements thermal conduction code ANSYS [6], giving as an input to the code the surface temperature distribution as measured from the camera. Fig. 3 shows the 2D finite elements model of one tile and the stainless steel support. At the interface between graphite and stainless steel a thermal contact resistance was considered [7,8]. It has already been checked, by changing the thermal resistance value in the simulation that its influence on the calculation of the λ_q is very small. The calculated flux impinging onto the wall has been corrected by subtracting the radiated power as measured from the bolometric diagnostic.

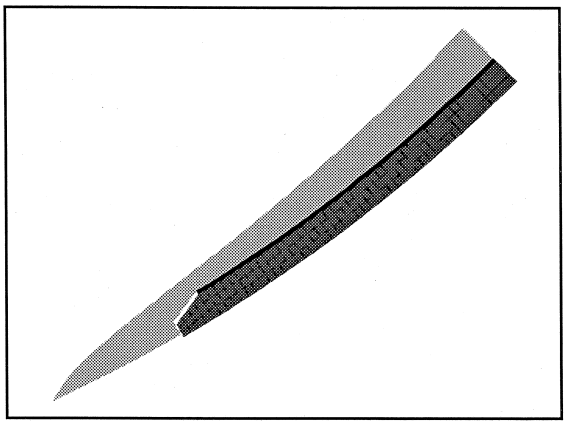

Fig. 3. The 2D finite element model of the tile used to calculate the power profile and its stainless steel support. The black oculars correspond to the thermal contact resistance. Its thermal conductivity was estimated from literature. A specific heat of 1 (J/g K) and a density of 1 (g/m^3) is assumed since the thermal contact resistance do not have thermal capacity. The light and dark grey elements correspond to graphite and stainless steel, respectively. In this figure, the element size is widened to show the mesh structure. The real element size used in simulation was estimated with an optimization procedure.

3.2. Thermal quench phase

Due to the very short duration of the thermal quench and to the very high graphite thermal conductivity during the reading of all the pixels of one full frame the limiter thermal pattern starts blurring. We had to apply a software algorithm to reconstruct the full pattern at the end of the thermal quench in order to calculate the λ_q. The image reconstruction was performed as follows: (1) first we measured the thermal quench duration by means of a fast (20 kHz) single point IR detector looking directly in the centre of the limiter blade imaged by our camera; (2) then we calculated the exact time delay between the end of the pixel integration phase and the end of the thermal quench for each pixel; (3) finally, by using a simple semi-infinite 1D solid heat conduction model we reconstructed the full temperature pattern at the end of the thermal quench. Assuming a constant heat flux during the thermal quench the temperature increment behaviour on the surface during the heat pulse is (for pixels integrating before the thermal quench end)

$$\Delta T = 1.1284\left[\frac{F_0(\sqrt{D}}{K}\right]\sqrt{t} \text{ for } t < t_1 \qquad (1)$$

and during the cooling phase (for pixels integrating after the thermal quench end) is

$$\Delta T = 1.1284\left[\frac{F_0(\sqrt{D}}{K}\right]\left(\sqrt{t} - \sqrt{t - t_1}\right) \text{ for } t > t_1, \qquad (2)$$

where F_0 is the heat flux, K the thermal conductivity, D the thermal diffusivity and t_1 the thermal quench duration.

The time duration of the event in the simulations has been slightly changed in order to take into account the possible measurement error; furthermore different heat flux time evolutions, as already found on this machine [9], have been simulated in order to check the influence of this parameter on the λ_q values; by combining these possible sources of errors we find out that the profile calculation accuracy is within 10%.

Such as for the stationary phase, we subtracted the radiated heat flux to the impinging flux. Since it was not possible to have a correct measurement of the radiated power during the thermal quench, we estimated it from the wall temperature increase in the neighbourhood of the limiter as measured by the camera.

4. Experimental results and discussion

A set of four disruptions extracted from a shot day completely dedicated to this phenomena have been analysed; two of them are density limit disruptions, one is obtained by impurity influx and the last is a low q disruption obtained by ramping down the current. The thermal fluxes are obtained at the thermal quench and in the stationary phase using two completely different calculation procedures, a conventional one during the stationary phase and reconstructing the pattern at a time during the thermal quench, as described in Section 3.2.

4.1. Heat flux profiles

Power deposition profile on one of the imaged tile is shown in Fig. 4 for a density limit disruption.

By using the magnetic configuration reconstruction just before the thermal quench the scalar product

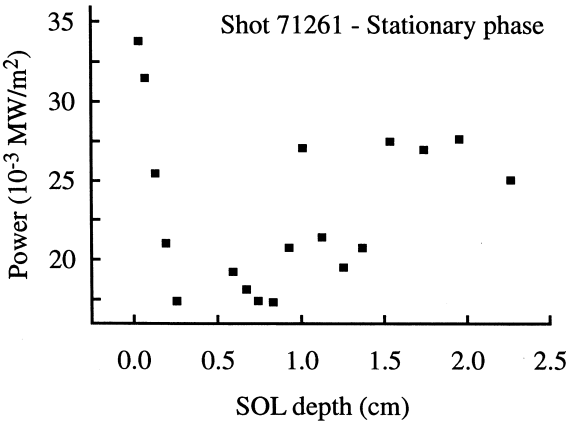

Fig. 4. Power deposition profile on the same tile of Fig. 3 during the stationary phase for a density limit disruption.

between the surface normal unit vector and the unit vector tangent to the magnetic line has been calculated for every pixel; In this way the profile of the heat flux vs. the scrape off layer thickness has been finally obtained.

The power flux profile during the stationary phase shows two different λ_q: in the region $0 < r - a < 0.4$ cm, where r is the radial coordinate and a the plasma minor radius, λ_q is of the order of a few millimetres; in the region $0.4 < r - a < 2.5$ cm λ_q is of the order of 1.5 cm (Fig. 5). During the stationary phase no changes with respect to this shape have been observed between shots with/without NBI and at different toroidal magnetic field values.

The same, unusual, two λ_q shape has been found also during the thermal quench phase (Fig. 6) for all the analysed disruptions. In the region between 0.4 and 2.5 cm the λ_q (1.5 cm) is equal for all the four disruptions.

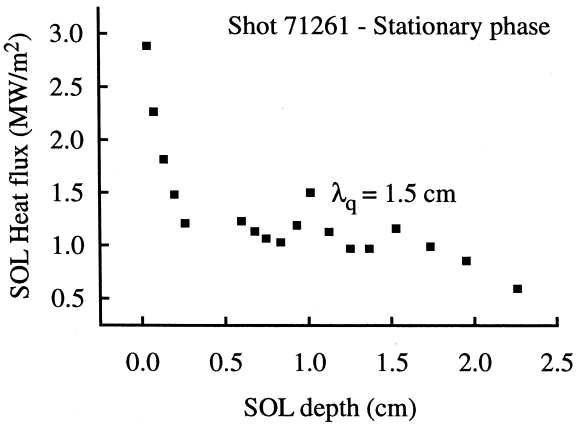

Fig. 5. The flux profile during the normal phase of the discharge. Minor displacements from a continuous shape are caused by a complex shadowing pattern due to the interaction between the magnetic ripple and the limiter shape.

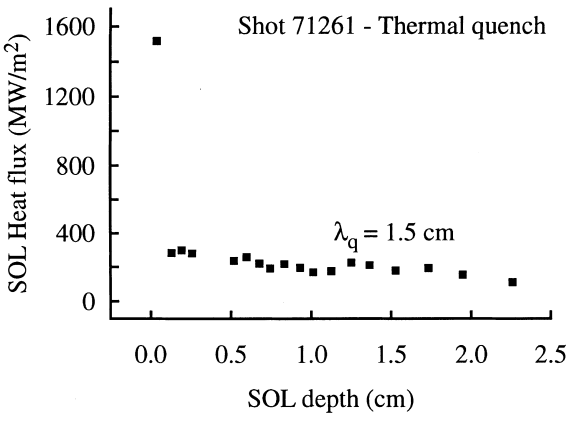

Fig. 6. The flux profile during the thermal quench phase of the discharge.

In the small region $0 < r - a < 0.4$ cm the λ_q also seems to be steeper (<1 mm) during the thermal quench. The quantitative comparison in this small region is more critical; errors in the incidence angle of the flux lines lead to bigger errors in the calculated flux because of the grazing incidence. It has also to be taken into account that the magnetic reconstruction is of course not available during the thermal quench.

A large part of the power flowing in the SOL seems to be lost onto the limiter in the region $r - a < 0.4$ cm. We think that it has been possible to see the enhancement of the profile close to the tangency point because of the current very high spatial and temperature resolution of our diagnostic compared to the previously installed one [10]. One pixel on the limiter corresponds roughly to 5 mm^2, and a fraction of a millimetre in terms of radial coordinate. We also think that the main source of error in the profiles arises from the low accuracy of the plasma magnetic reconstruction with respect to our camera spatial resolution. The physical explanation of such a profile is currently under discussion, but at least during the stationary phase the same profile has already been found by other IR diagnostics recently installed looking at the limiter. Finite Larmor radius effect and/or high electron temperature value close to the LCFS increasing parallel losses by enhanced electron thermal conductivity could be responsible for such a behaviour.

4.2. Energy deposition

Averaging the power flux profiles over the whole blade and multiplying by the total blade number, it is possible to calculate the power impinging onto the limiter both during the normal and the thermal quench phases. As already measured [5] the power collected by the limiter during the stationary phase represents around 40% of the plasma input power, while during the thermal quench of the analysed discharges we find that the value ranges between 40% and 90% of the diamagnetic plasma energy. We did not find a different trend in the energy deposited for the different kind of disruptions. Due to the modest number of discharges analysed it is difficult to rule out the possibility of a different behaviour for different kinds of disruptions.

Measuring from our images the temperature increase of the wall near the limiter and by extrapolating this value to the whole wall, we can also calculate the impinging power flux onto the wall during the thermal quench, by using the same analytical one-dimensional semi-infinite solid heat conduction model. In this way we calculated that the total energy deposited onto the wall ranges between 50% and 100% of the plasma energy content. Adding the energy flowing to the limiter for each of the analysed shots we obtained that the total power lost at the disruption ranges between 100% and 140% of the total plasma energy content.

We think that the main source of the over-estimation of this quantity is the flux on the wall being extrapolated from the measurements made in the vicinity of the limiter, where the radiative flux is probably enhanced by local high recycling.

5. Conclusions

Heat flux profiles with two different slopes have been found, also preserving their shape during thermal quench; the total energy released during this phase is comparable to the plasma energy content. No changes have been found for different kinds of disruptions (density limit, impurity influx, low q) but this may also be due to the modest number of discharges analysed.

References

[1] F.C. Schüller, Plasma Phys. Control. Fusion 37 (1995) A135.
[2] B.L. Newberry et al., ISFNT-3, Los Angeles, CA, 1994.
[3] M. Ciotti et al., Rev. Sci. Instrum. 68 (1997) 971.
[4] M. Ciotti et al., Elettro-ottica 96, Milano, 1996, pp. 251–255.
[5] M. Ciotti et al., Proc. 24th EPS, vol. 21A, Part IV, 1749.
[6] ANSYS, Swanson Analysis System, version 5.0.
[7] J.P. Holman, Heat Transfer 53, McGraw-Hill, New York, 1990.
[8] L.S. Fletcher, C.V. Madhusudana, Contact heat transfer – The last decade, AIAA J. 24(3) (1985) 510.
[9] K.H. Finken et al., Nucl. Fusion 32 (6) (1992) 915.
[10] K.H. Finken et al., J. Nucl. Mater. 162–164 (1989) 655.